LAUSANNE AIRH - SEMINAR - IAHR 1987
WAVE ANALYSIS AND GENERATION IN LABORATORY BASINS

ESTIMATION OF DIRECTIONAL WAVE SPECTRA BY THE MAXIMUM ENTROPY METHOD

O.U. NWOGU[1], E.P.D. MANSARD[2], M.D. MILES[2], M. ISAACSON[1]
[1]Dept. of Civil Engineering, University of British Columbia, Vancouver, British Columbia, Canada
[2]Division of Mechanical Engineering, Hydraulics Laboratory National Research Council of Canada Ottawa, Ontario, K1A 0R6, Canada

ABSTRACT: This paper discusses the application of the Maximum Entropy Method (MEM) to the estimation of directional wave spectra. The spreading function considered as the most reasonable, maximizes the entropy subject to constraints provided by the relationship between the spreading function and the input cross-spectral density matrix. The method is applicable to the measurement of various wave properties at a single location using a mixed instrument array.

A single summation, random phase method was used to numerically simulate directional sea states with varying degrees of noise and reflections in order to assess the accuracy and directional resolution of the MEM for a wave probe - biaxial current meter array. The analysis technique was also evaluated using physical simulations in the three-dimensional wave basin of the NRCC Hydraulics Laboratory. Finally the MEM was used to analyze field data obtained from the Canadian Coastal Sediment Study.

The MEM is compared with the extensively used Maximum Likelihood Method (MLM) for various random multi-directional sea states. The results indicate that the MEM resolves directional seas better than the MLM.

1.0 INTRODUCTION

The need for a more realistic reproduction of the ocean environment has led in recent years to the simulation of three-dimensional sea states in several laboratories around the world. The three-dimensional wave field has to be correctly resolved in order to understand the behaviour of coastal and offshore structures in such sea states.

The directional wave spectrum is often used to describe the energy distribution in a given sea state as a function of both wave frequency and direction. There are various methods which are presently used to estimate directional wave spectra. These include the direct Fourier transform method, parametric methods, the maximum likelihood method, the Fourier vector method, and the maximum entropy method.

The direct Fourier transform method first proposed by Barber [1] estimates the directional spectrum from the Fourier transform of the cross-spectra.

Parametric methods involve modelling the angular spreading function as either a truncated Fourier series or a distribution such as the cosine power or circular normal distributions. For the Fourier series approach, the Fourier coefficients are estimated from the relationship between the directional wave spectrum and the cross-spectral density of either the heave and slope signals of a floating buoy (Longuet-Higgins et al., [2]) or the water surface elevation from an array of wave gauges (Panicker, [3]).

The maximum likelihood method (MLM) was developed by Capon [4] for applications in geophysics. Oakley and Lozow [5] applied the method to directional wave resolution from an array of wave gauges. Isobe et al. [6] extended the method to include measurement of other wave properties such as velocities and slopes (EMLM). Jeffreys [7] compared the EMLM with parametric methods (cosine power and Fourier series) and found that the EMLM gave the best directional resolution of the three methods.

The Fourier vector method proposed by Sand and Lundgren [8] computes from measurements of the water surface elevation and orbital velocities the amplitudes, directions and phases for each of the Fourier components.

The maximum entropy method, which has its origins in probability theory (Jaynes, [9]), was subsequently developed for use in spectral analysis by Burg [10]. Barnard [11] attempted to extend Burg's method to the computation of wavenumber spectra, but an analytical solution could only be found for an equally-spaced linear array. The linear array, however, does not resolve directional seas adequately.

Kobune and Hashimoto [12] applied the MEM to the estimation of directional wave spectra from the measurements of various wave properties such as the water surface elevation and slope at a single location. The MEM was found to resolve directional seas better than the MLM. The only drawback of the MEM is that it is an iterative procedure and does not converge for very narrow spreading functions.

It should be noted that [12] employed the definition of entropy used in probability theory while [11] used the change in entropy, a definition currently used in spectral analysis. While an analytical solution can be found for the wave gauge-current meter array using the spectral analysis definition, it results in double peaked spreading functions satisfying the constraints imposed by the cross-spectral density matrix for unimodal seas, and is consequently not used in this paper.

In validating MLM and MEM techniques, most of the previous studies ([6], [7], [12]) simulate directly a cross-spectral density matrix representing a specified directional sea state. In any real situation, however, the data is usually available in the form of time series. Furthermore, the time series are generally corrupted to a certain degree by the presence of noise and reflections. It was therefore the intent of this study to use time series of the different wave properties to evaluate the effect of noise and reflection on the performance of the MEM.

2.0 DERIVATION OF THE MEM SOLUTION

The directional wave spectrum $S(f,\theta)$ is often represented by an angular spreading function applied to the conventional one-dimensional spectrum

$$S(f,\theta) = S(f) \cdot D(f,\theta) \tag{1}$$

where $S(f)$ is the frequency spectrum and $D(f,\theta)$ is the angular spreading function which is non-negative and should satisfy

$$\int_{-\pi}^{\pi} D(f,\theta)\, d\theta = 1 \tag{2}$$

For a spatially homogeneous wave field, the angular spreading function can be related to the cross spectra of the recorded time series. For measurements of the water surface elevation, η, and the two orthogonal horizontal velocities u and v, the following relationship exists

$$\int_{-\pi}^{\pi} D(f,\theta) \cdot \alpha_i(\theta)\, d\theta = \phi_i(f) \qquad i = 1,\ldots,5 \tag{3}$$

where

$$\left.\begin{aligned}
\phi_1(f) &= 1 && ; \quad \alpha = 1 \\
\phi_2(f) &= \frac{C_{\eta u}}{H(f) \cdot S_\eta(f)} && ; \quad \alpha_2 = \cos\theta \\
\phi_3(f) &= \frac{C_{\eta v}}{H(f) \cdot S_\eta(f)} && ; \quad \alpha_3 = \sin\theta \\
\phi_4(f) &= \frac{C_{uu} - C_{vv}}{H^2(f) \cdot S_\eta(f)} && ; \quad \alpha_4 = \cos 2\theta \\
\phi_5(f) &= \frac{C_{uv}}{H^2(f) \cdot S_\eta(f)} && ; \quad \alpha_5 = \sin 2\theta
\end{aligned}\right\} \tag{4}$$

where $C_{\eta u}$, $C_{\eta v}$, etc. are the co-spectra, while $H(f)$ is the transfer function relating the water surface elevation to the horizontal orbital velocity given by linear wave theory. Instead of using linear wave theory, $H(f)$ is often determined directly from the measured co-spectra as

$$H(f) = \sqrt{\frac{C_{uu} + C_{vv}}{C_{\eta\eta}}} \tag{5}$$

The entropy of the angular spreading function can be expressed as

$$I = \int_{-\pi}^{\pi} - D(f,\theta) \cdot \ln D(f,\theta)\, d\theta$$

Maximising the entropy function, I, subject to constraints given by equation (3) produces the solution

$$D(f,\theta) = \exp\left\{- \sum_{i=1}^{5} \mu_i \alpha_i(\theta)\right\}$$

where the parameters μ_i are Lagrange multipliers chosen to ensure that the estimate of the spreading function is consistent with the measured cross-spectral density matrix.

Substitution of the maximum entropy solution (7) into equation (3) results in a nonlinear set of equations

$$\int_{-\pi}^{\pi} \exp\left\{- \sum_{i=1}^{5} \mu_i \alpha_i(\theta)\right\} \alpha_i(\theta)\, d\theta = \phi_i(f) \qquad i = 1,\ldots,5 \quad (8)$$

An analytical solution for the above parameters μ_i cannot be easily determined so one has to resort to an iterative technique such as the Newton-Raphson procedure. These equations are similar to those derived in [12] except that μ_1 is retained here as an iteration parameter to improve convergence for narrow spreading functions, while [12] used only the last four multipliers.

A suitable initial guess for the parameters μ_i can be determined from the MLM solution $D(\theta)$ as

$$\mu_1 = - \frac{1}{\pi} \int_{-\pi}^{\pi} \ln D(\theta)\, d\theta$$

$$\mu_i = - \frac{2}{\pi} \int_{-\pi}^{\pi} \ln D(\theta) \cdot \alpha_i(\theta)\, d\theta \qquad i = 2,\ldots,5 \quad (9)$$

For unimodal symmetric distributions, the following circular normal distribution proposed by Borgman [13] gives a good approximation of the maximum entropy solution

$$D(\theta) = \exp\left\{\mu\cos(\theta - \theta_m)\right\} / 2\pi I_0(\mu) \quad (10)$$

where I_0 is the modified Bessel function of the first kind, of order zero. The mean direction, θ_m, is given by

$$\theta_m = \arctan\,(\phi_3/\phi_2) \quad (11)$$

while μ is chosen to satisfy two constraints (i = 2,3) of equation (3)

$$\frac{I_1(\mu)}{\pi I_0(\mu)} = \phi_2 \cos\theta m + \phi_3 \sin\theta m \quad (12)$$

A suitable check should however be applied to determine whether the distribution is unimodal or bimodal. One such check is the parameter β defined by

$$\beta = \frac{\phi_2 \cos\theta m + \phi_3 \sin\theta m}{\phi_4 \cos 2\theta m + \phi_5 \sin 2\theta m} \tag{13}$$

$\beta \geq 1$ indicates a unimodal sea, while $\beta < 1$ indicates a bimodal sea.

3.0 NUMERICAL SIMULATIONS

Miles and Funke [14] have compared various numerical models for the synthesis of directional seas. One model which produces a spatially homogenous wave field is the single direction per frequency model. The water surface elevation is given by

$$\eta(x,y,t) = \sum_{i=1}^{N} A_i \cos\left[2\pi f_i - k_i(x \cos\theta_i + y \sin\theta_i) + \varepsilon_i\right] \tag{14}$$

where A_i and ε_i are the amplitudes and phases of the wave components given by the random phase method as

$$A_i = \sqrt{2S(f_i)\ D(f_i,\theta_i)\Delta f \Delta\theta} \tag{15}$$

$$\varepsilon_i = 2\pi\ U[0,1]$$

where $f_i = i(\Delta f/M)$ and $U[0,1]$ is a uniform distribution from 0 to 1. θ_i are chosen by a procedure such that the spreading function is approximated by M wave angles in each frequency band of width Δf. One such procedure is that in which the wave angle increases linearly with frequency

$$\theta_i = \theta_0 + (i - 1)\Delta\theta - \theta_{max} \tag{16}$$

where $\Delta\theta = 2\theta_{max} / (M - 1)$ and θ_{max} is the maximum spreading angle. The synthesized frequency spectrum will match the target spectrum at a frequency resolution Δf or larger, and the cross-spectra are reasonably accurate for $M > 32$. The horizontal orbital velocity is always in phase with wave elevation and in the direction of propagation of the sinusoidal wave component. The amplitudes of orthogonal velocity components are given by

$$\begin{Bmatrix} u_i \\ v_i \end{Bmatrix} = A_i \cdot H(f_i) \begin{Bmatrix} \cos\theta_i \\ \sin\theta_i \end{Bmatrix} \tag{17}$$

A Bretschneider wave spectrum was used for the synthesis with a frequency independent cosine power spreading function of the following form

$$D(\theta) = \frac{\sqrt{\pi}\ \Gamma(s+1)}{2\theta_{max}\Gamma(s+0.5)} \left|\cos\left[\frac{\pi\ (\theta - \theta_m)}{2\theta_{max}}\right]\right|^{2s} \qquad |\theta - \theta_m| < \theta_{max} \tag{18}$$

The parameter s is a spreading index describing the degree of short-crestedness of the wave field. Different spreading indices varying from s = 1 to s = 50 were used with a θ_{max} value of 90°. The time series were synthesized at a time interval of 0.2 s, with 64 wave angles in each frequency band of 0.04 Hz resulting in a record length of 1638.4 s.

In order to examine the effect of noise on the directional resolution of the MEM and MLM, a noise signal representing a white noise spectrum with constant spectral density from zero to the Nyquist frequency was added to the simulated time series. The root mean square (rms) noise amplitude was set equal to a specified percentage of the rms amplitude of the water surface elevation and velocity data. The time series of the noise component were generated by the inverse FFT of the white noise amplitude spectrum and a randomly selected phase spectrum. Different phase spectra were used for the different wave properties in order to make them uncorrelated.

Since both the MLM and MEM techniques are based on the assumption of a spatially homogenous sea state, it was proposed in this paper to investigate the degree of error caused by possible spatial non-homogeneity. In laboratory basins or coastal regions, a certain amount of reflection is always present. The reflected wave and incident wave components, being of the same frequency, are "phase locked" resulting in a spatially non-homogenous wave field. The reflected wave component can be expressed as

$$\eta_R(x,y,t) = C_r \cdot A_i \cos\left\{\omega_i t - k_i\left[(2x_R - x)\cos\theta_i + y\sin\theta_i\right] + \varepsilon_i\right\} \quad (19)$$

where C_r is the reflection coefficient and x_R is the x-coordinate of the reflecting boundary.

4.0 ANALYSIS OF NUMERICALLY SIMULATED DATA

4.1 Effect of Noise

The MEM and MLM were used to analyze the numerically simulated time series of the water surface elevation and horizontal orbital velocities for specified directional spreading functions.

The cross spectral density matrices were obtained by the FFT of overlapped windowed segments of the time series. For this purpose a 50% segment overlap and a cosine window were applied. The frequency resolution used in the simulation was also used in the analysis.

Figure 1(a) shows the target wave elevation spectrum and the synthesized wave elevation and horizontal in-line and transverse velocity spectra. The wave elevation spectrum has a significant wave height, H_{m0} = 0.4 m and a peak frequency, f_p = 0.4 Hz. The velocity spectra are shown for s = 10 with θ_m = 60°. As expected, the random phase synthesized spectrum matches the target spectrum fairly well. The small differences are due to the segment averaging method used for the spectral analysis.

Figure 1(b) shows the mean direction obtained by the MEM method as a function of frequency for the case of s = 10 with 0%, 10%

and 20% noise. Since the MLM analysis also showed the same behaviour of mean direction versus frequency for the different levels of noise, the results are not shown here. It can be seen that at the low and high frequency tails of the spectrum, the estimated mean direction starts to deviate from the expected value. At $f = 2.5f_p$ (1.0 Hz), θ_m increases to 61.4° for 10% noise and 64.8° for 20% noise. Since the noise spectrum was synthesized to be constant over the entire frequency band, the signal to noise ratio becomes very low at the low and high frequency tails of the spectrum where there is little energy. This affects the estimated cross-spectral matrix components and hence degrades the resolution of both the MEM and MLM. Similarly, the noise also affects the estimate of the directional spread defined by

$$\sigma_\theta(f) = \left[\int_{\theta_m-\pi/2}^{\theta_m+\pi/2} D(f,\theta)\ (\theta - \theta_m)^2\ d\theta \right]^{1/2} \qquad (20)$$

Figures 1(c) and (d) show the directional spread obtained by the MEM and MLM respectively for s = 10 with 0%, 10% and 20% noise. The expected directional spread is 12.5°. For 0% noise, the MEM estimates the directional spread very well while the MLM results deviate by about 26.5% at $f = f_p$. This is because the MLM estimated directional spreading function does not have to satisfy the constraints (equation (3)) of the original cross-spectral density matrix.

Even with as much as 20% noise, the MEM estimate of the directional spread is quite acceptable (less than 10%) over the frequency range 0.75 f_p to 1.5 f_p. However, at the higher and lower frequencies where the energy content is low, substantial differences can be found. At $f = 2f_p$ for instance, the directional spread deviates by as much as 34% and 147% for the MEM and MLM respectively.

Figures 1(e) and (f) show the expected, MEM and MLM estimated spreading functions for s = 1 and s = 30, respectively with 0% noise at $f = f_p$. It can be seen that the MEM estimates the spreading function better than the MLM for both cases. Computations indicate that for $s \geq 5$, the MEM estimated and expected spreading functions are virtually indistinguishable for 0% noise. This is much in line with the results previously obtained by [12].

Figures 1(g) and (h) show the spreading functions obtained for s = 10 with 20% noise at $f = f_p$ and $f = 2f_p$, respectively. It can be seen that even with 20% noise, the MEM still estimates the spreading function accurately at the peak frequency. At twice the peak frequency, the distribution becomes broader but the mean direction is still well estimated. For frequencies equal to or higher than twice the peak frequency at 20% noise, the MEM starts detecting a spurious second peak (at −120° in this case).

The use of five Lagrange multipliers in the iteration procedure instead of the four used by [12], and the MLM solution as an initial guess, ensures convergence of the solution for values of s up to 50. This is significantly higher than the maximum s = 5 (based on $\theta_{max} = 90°$) or s = 20 (based on $\theta_{max} = 180°$) obtained by [12]

without specifying the initial values of the parameters by trial and error. For s values greater than 50, the wave field can essentially be considered long-crested for most practical applications.

4.2 Effect of Reflecting Boundary

Numerical simulations of a directional sea state with a reflecting boundary located at distances of half a wavelength and a quarter of a wavelength from the wave gauge-current meter array were also carried out. The wavelength was based on the peak frequency of the wave spectrum. These distances were chosen so that the measurement location would represent approximately an anti-nodal and a nodal position respectively.

Figures 2(a) and (b) show the spreading functions obtained with s = 10 at the peak frequency, for a reflection coefficient of 30%. The simulations were carried out for 0% noise and a mean incident direction of 30°. At the antinode, the wave spreading function of the incident wave is fairly well estimated by the MEM while the MLM estimates a wider distribution. The MEM does detect a reflected wave field, but its distribution is too broad and centred at 180° instead of 150°. The MLM does not detect the reflected wave field. When the location of the measurement array was simulated at a nodal position, both the MEM and MLM estimate spreading functions for the incident wave much narrower than expected (Figure 1(b)). The estimate of the mean incident direction is also in error by 10°. The MEM detects a narrower reflected wave field centred at 140° instead of 150°. These figures clearly show the effect of phase locking on the resolution of the MEM and MLM. In such a wave field, the relationship between the cross-spectral density matrix and the spreading function (equation (3)) is no longer valid but would have to be modified to take into account the distance to the reflecting boundary. Isobe and Kondo [15] modified the MLM technique for a wave probe array to take into account phase interaction terms in an incident and reflected wave field. A similar approach can be used for a mixed instrument array at a single location.

Figure 2(d) shows the frequency dependence of the expected and MEM estimated mean directions of the incident and reflected wave components and directional spread of the incident wave component for the nodal location. Since the nodal position is based on the peak period of the wave, substantial differences can be found at $f = f_p$. An additional set of investigations was carried out, this time by interlacing the frequencies of the incident and reflected wave components. This resulted in a homogeneous sea state, with no correlation of wave energy from different directions. The MEM was then able to accurately resolve such a bi-directional sea state (Figure 2(c)).

4.3 Analysis of Bimodal Seas

Figure 3(a) shows a bimodal sea state simulated with local sea and swell components. The significant wave height, peak period, spreading index and mean direction are shown in the figure. Figure 3(b) shows the target and synthesized frequency spectra. The target wave spectrum is fairly well reproduced by the single summation, random phase method. Figures 3(c) and (d) show the spreading functions ob-

tained at the peak frequencies of the swell and local sea. It can be seen that the MEM estimates the specified spreading functions accurately.

5.0 ANALYSIS OF LABORATORY AND FIELD DATA

The MEM was also used to analyse data obtained in the three-dimensional offshore wave basin of the NRCC. A detailed description of the facilities can be found in Miles et al. [16]. Tests were carried out using a Bretschneider wave spectrum with H_{m0} = 0.4 m, f_p = 0.4 Hz and known directional characteristics, in water of depth 2 m. An instrumentation package consisting of a wave probe and two Marsh McBirney biaxial current meters placed at elevations (Z_{cm}) of 1.08 m and 1.68 m above the basin floor, was set up 9 m away from the wave generator. Data was collected at a sampling frequency of 10 Hz for 409.6 s. The data was analysed at a frequency resolution of 0.04 Hz.

Figure 4(a) shows the expected wave elevation, measured wave elevation, and horizontal velocity spectra for s = 5 with θ_m = 0°. Figure 4(b) shows the MEM and MLM estimated directional spread for the two current meters. The expected directional spread is 17.25°. In the vicinity of the peak frequency, the MEM estimates the spread fairly well. At the low and high frequency tails, the estimated distributions become broader. This is partly because there is very little energy in the velocity spectra for f < 0.27 Hz and f > 0.8 Hz. The cross-spectral density matrix estimates would thus be corrupted in that region.

Figures 4(c) and (d) show the directional spreading functions obtained for s = 5 and s = 1 at the peak frequency for the upper current meter. It can be seen that the directional sea state generated in the basin for s = 5 matches the specified sea state at the peak frequency. For the broader distribution s = 1, the mean direction tends to be slightly shifted and the distribution distorted. This may be partly due to wave propagation characteristics in the basin. Judging from the lack of secondary peaks, it can be assumed that there is very little reflection from the side beaches installed around the basin.

The MEM was also used to analyse some data obtained from the Canadian Coastal Sediment Study. Part of the Study was carried out at Stanhope Lane, Prince Edward Island in the autumn of 1984. The orbital velocities were measured with two Marsh McBirney biaxial current meters located at elevations of 24 cm and 54 cm above the seabed in water depths varying from 2 m to 3 m. The positive x axis of the current meter was oriented 30° east of north. A pressure sensor was also placed on the instrumentation stand at a height of 70 cm above the seabed. Data was collected at a sampling frequency of 5 Hz for a duration of 20 min yielding 6,000 data points (see Bowen et al. [17]).

The recorded time series were analysed at a frequency resolution of 0.01 Hz. Figure 5(a) shows the spectra of the wave elevations and horizontal orbital velocities measured on the 29th of October 1984 at 16:00 hrs. The storm had a significant wave height of 0.6 m and a peak period of 4.7 s.

Figure 5(b) shows the spreading function obtained at the peak frequency for the upper current meter. The spreading function is bi-

directional with a mean incident wave direction towards the shore and a mean reflected wave direction away from the shore. The reflection coefficient estimated from the spreading function is 40%. The reflection coefficient is quite high because the instrumentation package was placed on a sand bar. There was also a second sand bar located further towards shore.

Figures 5(c) and (d) show the incident and reflected wave mean directions and directional spread obtained from the two current meters by the MEM. Both quantities do not display the oscillatory behaviour showed by the numerically simulated reflected wave field. It is thus believed that phase locking might not have been predominant in this case due to diffraction, refraction and nonlinear effects in shallow water.

6.0 CONCLUSIONS

The maximum entropy method has been applied successfully to the estimation of directional wave spectra from a wave probe-biaxial current meter array. The MEM yields a directional spreading function which is consistent with the input cross-spectral density matrix.

An extensive numerical simulation of various random multi-directional sea states was carried out with varying degrees of noise and reflections. Addition of noise to the signals degrades the resolution of the MEM and MLM at the low and high frequency tails of the spectra where the noise to signal ratio is high.

In a reflected or crossing wave field, there is phase locking of individual wave components and the MEM should no longer be used unless the constraint equations are modified to take into account the spatial variability.

The MEM was compared with the MLM for unimodal as well as bimodal seas and it was shown that the MEM consistently resolves directional seas better than the MLM. Even at 20% noise, the MEM estimate of the directional spread is in error by less than 10% in the frequency range $0.75f_p$ to $1.5f_p$ for spreading index, s = 10 while the MLM estimate deviates by 26.5% at $f = f_p$ for 0% noise.

7.0 REFERENCES

1. BARBER, N.F., (1963), "Directional Resolving Power of an Array of Wave Detectors", Ocean Wave Spectra, Prentice-Hall, New Jersey, pp. 137-150.

2. LONGUET-HIGGINS, M.S., D.E. CARTWRIGHT and N.D. SMITH, (1963), "Observations of the Directional Spectrum of Sea Waves Using the Motions of a Floating Buoy", Ocean wave Spectra, Prentice-Hall, New Jersey, pp. 111-132.

3. PANICKER, N.N., (1971), "Determination of Directional Spectra of Ocean Waves from Ocean Arrays", Hydrogr. Eng. Lab. Rep. HEL1-18, University of California, Berkeley.

4. CAPON, J., (1969), "High Resolution Frequency Wavenumber Analysis", Proc. IEEE, Vol. 57, No. 8, pp. 1408-1418.

5. OAKLEY, O.H. and J.B. LOZOW, (1977), "Directional Spectra Measurement by Small Arrays", Proc. Offshore Tech. Conf., Houston, Paper No. OTC 2745, pp. 155-166.

6. ISOBE, M., K. KONDO and K. HORIKAWA, (1984), "Extension of MLM for Estimating Directional Wave Spectrum", Proc. Symp. on Description and Modelling of Directional Seas, Copenhagen, Denmark.

7. JEFFREYS, E.R., (1986), "Comparison of Three Methods for Calculation of Directional Spectra", Proc. 5th Int. Offshore Mechanics and Arctic Engineering Symp., Tokyo, Japan, Vol. I, pp. 45-50.

8. SAND, S.E. and H. LUNDGREN, (1979), "Three-Dimensional Structure of Ocean Waves", Proc. 2nd Int. Conf. on the Behaviour of Offshore Structures, BOSS '79, London, Vol. I, pp. 117-120.

9. JAYNES, E.T., (1957), "Information Theory and Statistical Mechanics", Papers I and II, Phys. Rev., Vols. 106 and 108.

10. BURG, J.P., (1967), "Maximum Entropy Spectral Analysis", Proc. 37th Annual Int. Soc. Explor. Geophys. Meeting, Oklahoma City.

11. BARNARD, T.E., (1969), "Analytical Studies of Techniques for the Computation of High-Resolution Wavenumber Spectra", Texas Instruments Advanced Array Research Spec. Rep. No. 9.

12. KOBUNE, K. and N. HASHIMOTO, (1986), "Estimation of Directional Spectra from the Maximum Entropy Principle", Proc. 5th Int. Offshore Mechanics and Arctic Engineering Symp., Tokyo, Japan, Vol. I, pp. 80-85.

13. BORGMAN, L.E., (1969), "Directional Spectra Models for Design Use", Proc. Offshore Tech. Conf., Paper No. OTC1069.

14. MILES, M.D. and E.R. FUNKE, (1987), "A Comparison of Methods for Synthesis of Directional Seas", Proc. 6th Int. Offshore Mechanics and Arctic Engineering Symp., Houston, Vol. II, pp. 247-255.

15. ISOBE, M. and K. KONDO, (1986), "Method for Estimating Directional Wave Spectrum in Incident and Reflected Wave Field", Proc. 19th Int. Coastal Eng. Conf., Houston, pp. 467-483.

16. MILES, M.D., P.H. LAURICH and E.R. FUNKE, (1986), "A Multi Mode Segmented Wave Generator for the NRC Hydraulics Laboratory", Proc. 21st American Towing Tank Conference, Washington, D.C.

17. BOWEN, A.J. et al., (1986), "Canadian Coastal Sediment Study - Final Report of the Steering Committee", Hydraulics Laboratory Technical Report TR-HY-013, National Research Council of Canada, Ottawa, Canada.

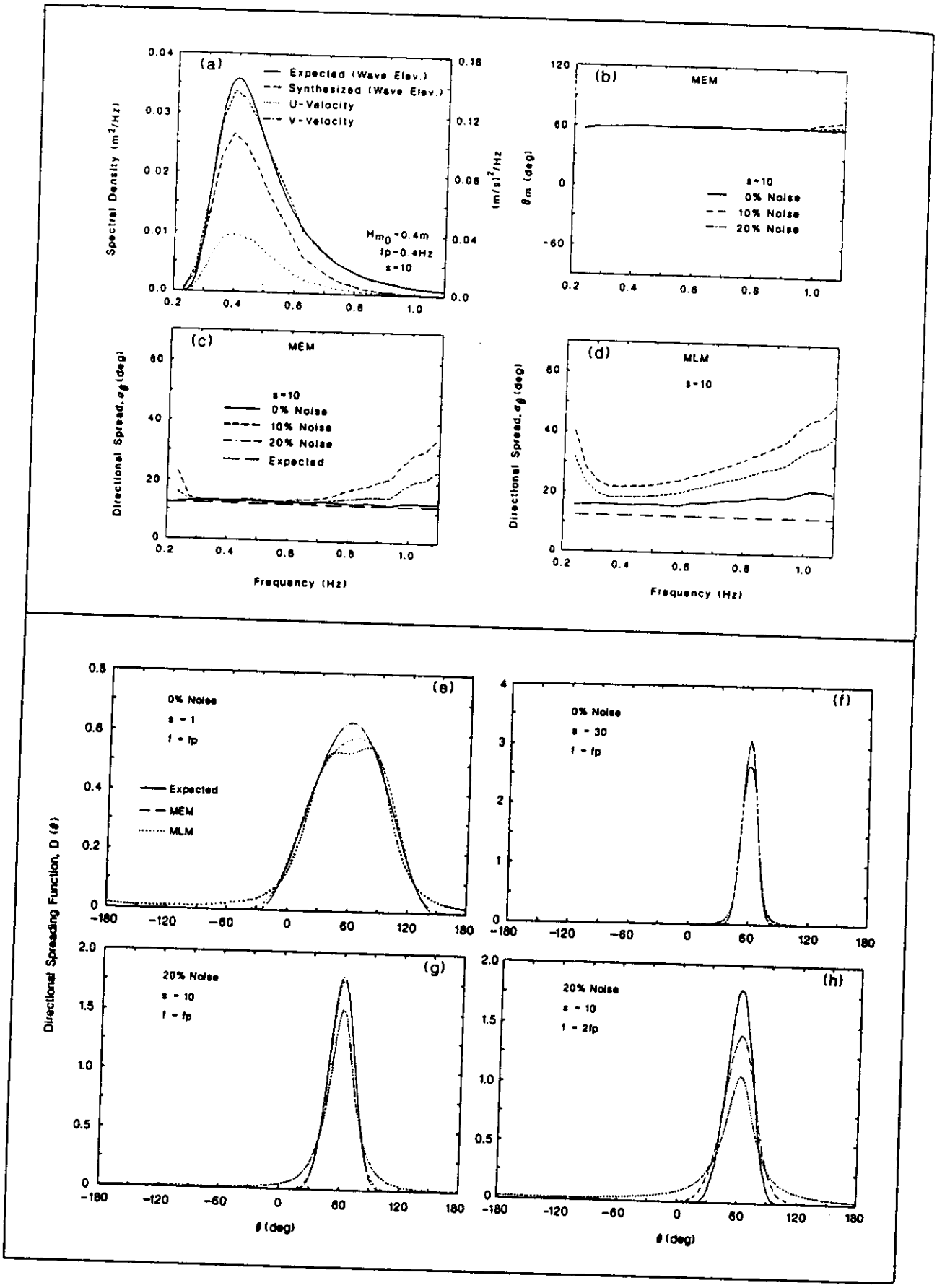

FIGURE 1 ANALYSIS OF DIRECTIONAL SEA STATES SIMULATED WITH DIFFERENT DEGREES OF NOISE

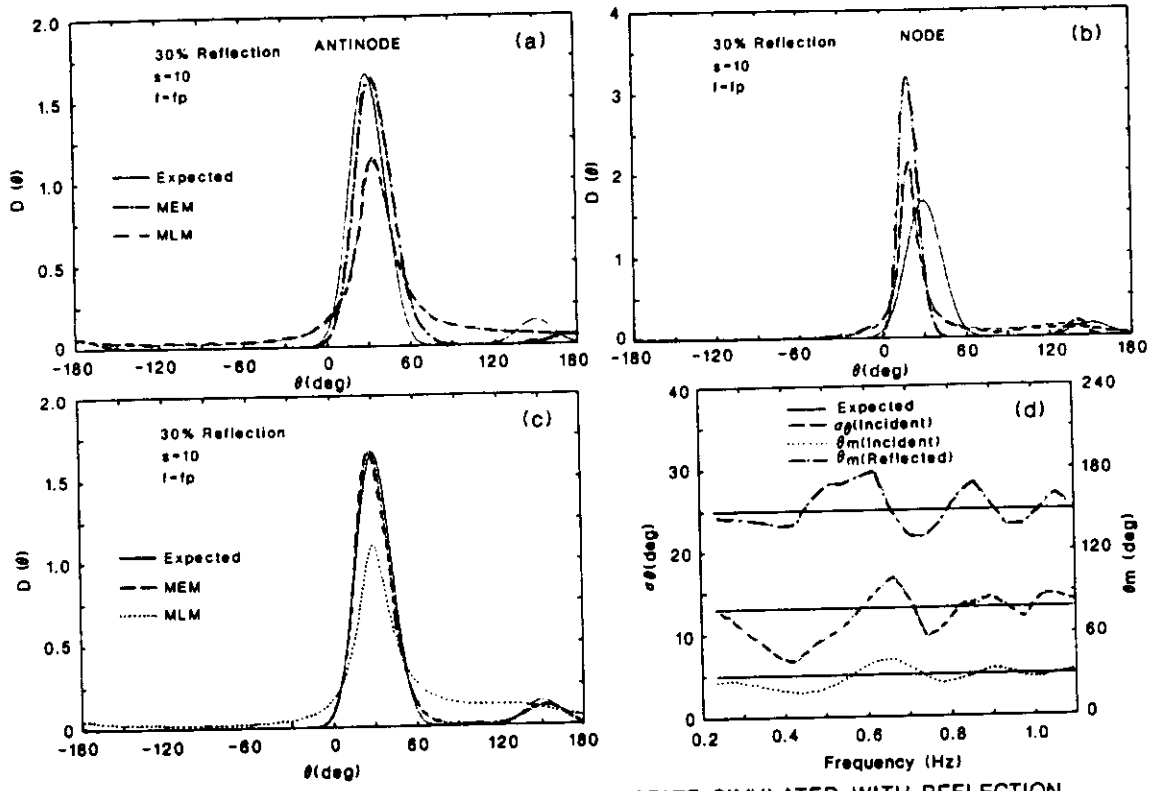

FIGURE 2 ANALYSIS OF A DIRECTIONAL SEA STATE SIMULATED WITH REFLECTION

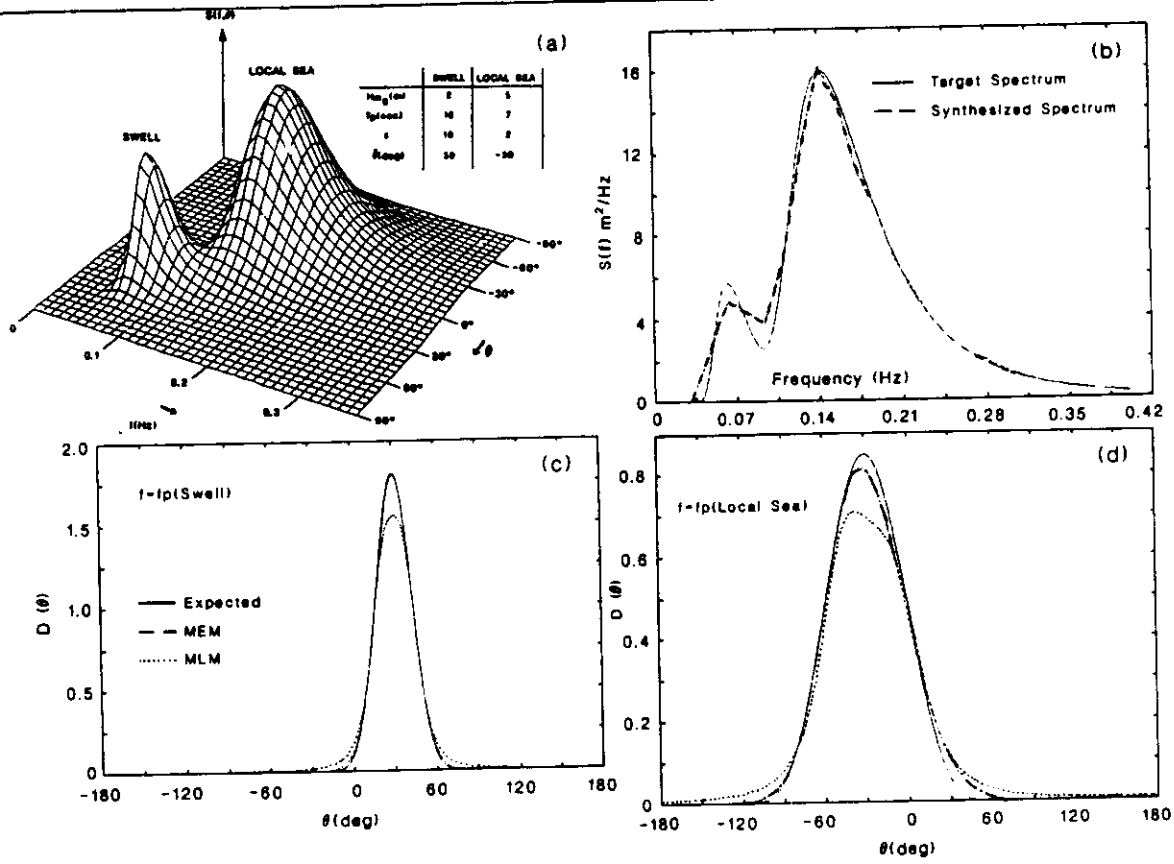

FIGURE 3 ANALYSIS OF A BIMODAL SEA STATE

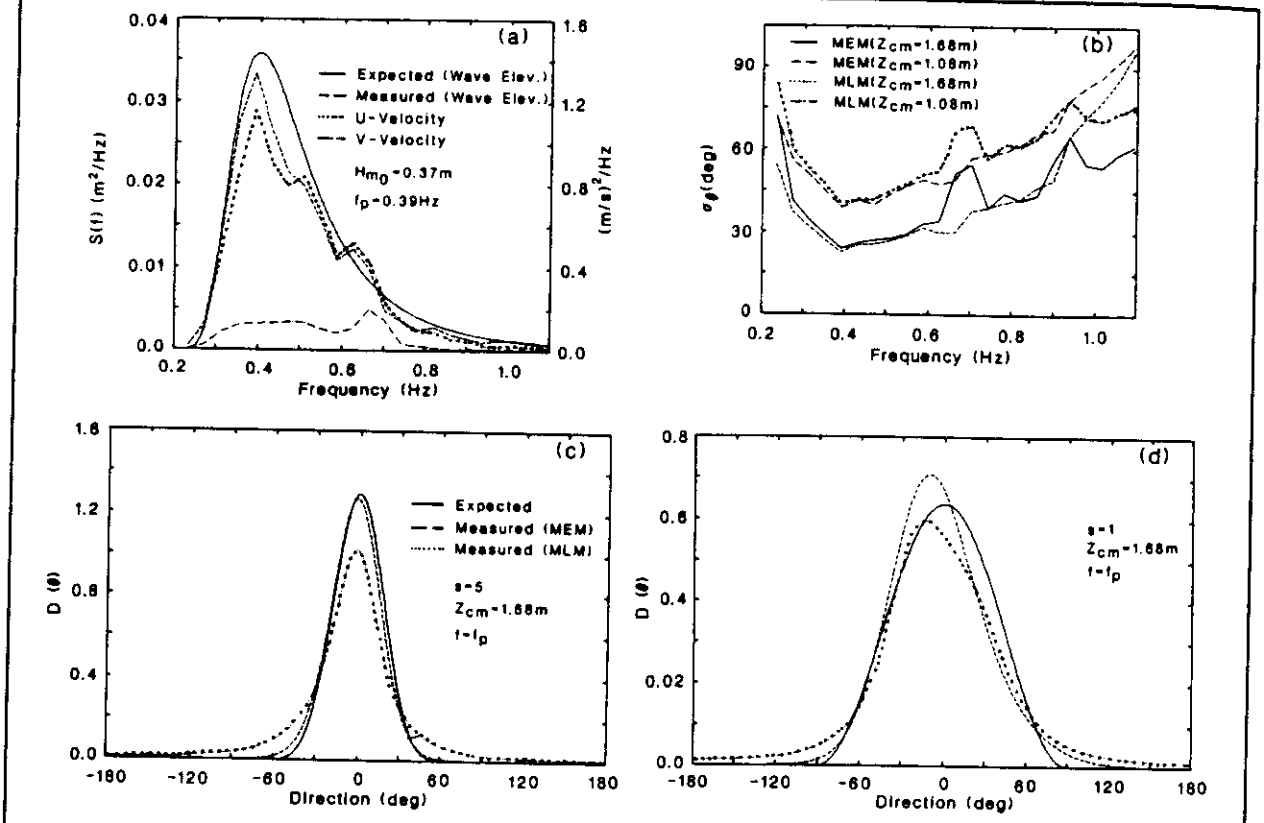

FIGURE 4 ANALYSIS OF LABORATORY DATA

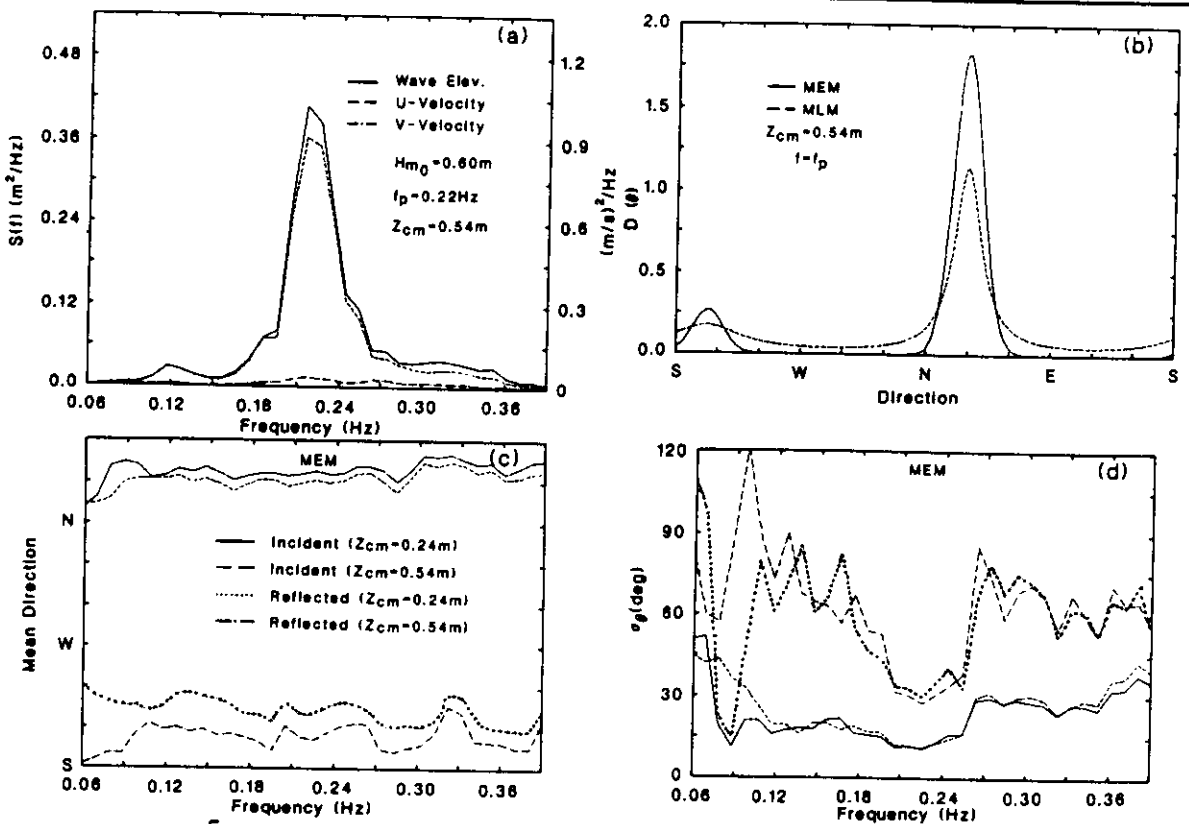

FIGURE 5 ANALYSIS OF FIELD DATA (STANHOPE LANE, PEI) 29/10/84 AT 16:00 HRS